Applications of Spatial Statistics and Spatial Analysis in Flooding Assessment Using GIS: A Case Study in Darab Watershed, Iran

Mohsen Shariati
University of Tehran Faculty of Environment
Mohamad Kazemi
Hormozgan University
Reza Naderi Samani
Soil Conservation and Watershed Management Research
Abdullah Kaviani Rad (akaviani2020@yahoo.com)
Shiraz University School of Agriculture

Research Article

Keywords: Spatial analysis, Spatial statistics, Flooding, Hazard, ArcGIS Pro

Posted Date: March 16th, 2022

DOI: https://doi.org/10.21203/rs.3.rs-1403115/v1

Abstract

Floods are amongst the most catastrophic natural disasters, having enormous impacts on both infrastructure and humans. Between 1998 and 2017, this detrimental phenomenon afflicted more than two billion individuals globally. The present investigation utilized two phases of spatial analysis and spatial statistics from ArcGIS in order to precisely assess the hazard of flooding in the Darab watershed, Iran. Following a survey of literature and case studies, seven criteria for flood risk were recognized to be effective: dem, slope, drainage density, NDVI, land cover, geology, and rainfall. The initial phase was operated using fuzzy logic and AHP in order to overlap layers. In order to prepare of flood hazard mapping, kernel density and zonal statistics were used to compute flood hazard density and flood hazard zoning. In flood hazard zones, spatial statistics in ArcGIS Pro were applied to detect high-and low-risk clusters. An innovation in this study is the use of local data to detect high-risk and low-risk flood clusters. According to the findings, the Gamma operator (0.9) was recognized as the optimal operator for flooding zoning, and only 7344/63432 hectares of the study area had a high risk of flooding, with only two high-risk flooding clusters in the Darab watershed. The boundary was near the heights in the north and northeast of the study, which corresponded to townships with a population of less than 5,000 people. Overall, the findings of this study demonstrated that clusters and outliers' analysis, as well as hotspot analysis, are effective complementary techniques to recognize high- and low-risk flood clusters. Combining spatial analysis with spatial statistics may be a reliable and efficient approach for natural scientific investigations.

1. Introduction

Floods, as one of the most catastrophic natural disasters, cause significant economic and human losses, affecting over two billion people globally between 1998 and 2017 (WHO, 2021). Floods were responsible for 43% of the 7255 natural disasters documented during 1998–2017 (UNISDR and CRED, 2018). Every year, this phenomenon costs countries billions of dollars and kills hundreds of people (Demir and Kisi, 2016). Due to global concerns regarding an increase in natural disasters, numerous studies have been conducted to evaluate various aspects of the origin and risk assessment of floods since the early twentieth century (Svetlana et al., 2015). Park and Won (2019) assessed flooding risk by surveying environmental factors across several sites with the objective of lowering urban flash flooding. Pham et al. (2021) investigated 84 flood hazard spots in Guang Nam province, Vietnam. Additionally, Khoirunisa et al. (2021) examined data from 307 floods that occurred in Keelung, Taiwan, between 2015 and 2019. Following their conclusions, the principal causes of flooding are rapid snowmelt, extreme rainfall, tsunamis, altitude, steep slopes, and poor drainage (WHO, 2021; Rincón et al., 2018; Ogato et al., 2020). Along with environmental factors, human activities such as deforestation, land-use change, industrialization, soil erosion, and climate change intensify flood phenomena and their corresponding consequences. Given the significant temporal and spatial variability of flood events, a systematic and continuous spatial and temporal evaluation of flood hazard, as well as an awareness of its drivers, is critical for flood management (Tang et al., 2021). Flood hazard assessment enables researchers to

pinpoint the probability of a flood occurring in a particular location or time frame (Argaz et al., 2019). This assessment requires an examination of the physical and geographical characteristics of flood inducers (Tanoue et al., 2016). In this regard, a study by Pourghasemi et al. (2020) noted the significance of spatial modeling of flood phenomena. Organizing a flood susceptibility map is critical for addressing this perilous occurrence (Saha et al., 2021). Floodwater zoning maps are predominantly used to provide vital information for disaster management.

Remote sensing (RS) and geographic information system (GIS) can offer a critical appraisal of the potential for flood hazards in the short timeframe required to generate a zonation map. Psomiadis et al. (2021) employed RS and GIS to assess the flood hazard on the Aegean Sea's southernmost island. Additionally, Osei et al. (2021) utilized a GIS-based framework for analyzing flood hazard areas in Ghana's Tarkwa mine area and found that 42.59% of the studied area was exposed to flooding. Rahmati et al. (2016) reported that the AHP method is incredibly efficient for accurately predicting flood risk and that both the AHP and GIS methods are appropriate for examining the potential for flood hazard, particularly in areas with limited data. Msabi and Makonyo (2021) demonstrated that preventing floods is unattainable due to climate change. On the other hand, attempting to create a flood susceptibility map can help alleviate flood impacts. Cities as the most at-risk sites should be examined on a continual basis, and flood zone maps and mitigation strategies should be addressed. (Rincón et al., 2018). It is reported that cities increase the ground impermeable layer, raising the risk of flooding by lowering the hydrological response time (Feng et al., 2021). Along with metropolitan regions, villages are at risk of severe flooding owing to a lack of vulnerability assessment (Desalegn and Mulu, 2021). According to Liu et al. (2020), floods are a substantial threat to rural China. Commercial and entertainment opportunities are available in the floodwatersheds and locations near rivers. However, they are always at risk of flooding. Therefore, developing rural areas adjacent to rivers and watersheds regardless of the hydrological and dynamic circumstances increases the risk of flooding and associated effects. Heavy and unexpected precipitation in arid and semi-arid areas results in floodwaters, which can be extremely catastrophic (Ghazavi et al., 2012).

Iran, as one of the world's arid and semi-arid regions, has experienced frequent floods during the last two decades (Modarres et al., 2016). Annually, enormous and detrimental floods occur in Iran as a result of the wide area and significant temporal and geographical variability of precipitation in the majority of basins, having a devastating impact on the country's towns and natural ecosystems (Arabameri et al., 2019). Iran experiences approximately 40 floods every year, and the frequency of floods and the corresponding damage are rising in the majority of watersheds. The August 2019 flood catastrophe in Iran affected 28 provinces (WHO, 2019), killed 210 people, and caused $31 million in damage. As a result, the dynamics of flood risk in Iran have recently attracted the attention of hydrologists and specialists in watershed management, resulting in the presentation of a considerable number of scientific papers. Maryanaji et al. (2020) determined the flood danger in Hamadan province based on its climatic characteristics. Arabameri et al. (2019) employed statistical multiple-criteria decision-making to determine the sensitivity of flood hazard in northern Iran and concluded that variables such as slope, distance to flood flow, land cover, and vegetation all play a significant role in flood generation.

Fars province, located in southern Iran, is at a significant risk of natural disasters such as earthquakes and floods due to its unique geographical characteristics and changeable weather conditions. Darab is one of the cities in Fars province that has considerable flood risks, as urban flash flooding imposes substantial damage to urban infrastructure. However, limited investigations have addressed flooding vulnerability and risk assessments in this region. Accordingly, this study attempts to (i) characterize the flood zone of the Darab watershed by analyzing slope, NDVI, land cover, geology, precipitation, drainage density, DEM, and distance from the river; and (ii) identify the spatial distribution pattern of flood hazard according to the residential areas and its relationship with land cover using the tools of spatial statistics and spatial analysis in ArcGIS Pro.

2. Materials And Methods

2.1. Study area

Darab city is located in Fars province's southeast region and has a population of approximately 201489 people. Darab has an area of around 7500 square kilometers and rises to an elevation of 1180 meters above sea level. The majority of Darab is characterized by a tropical climate, with precipitation mostly in the form of rain and totaling less than 350 millimeters per year. The Darab watershed and its elevations cover an area of 894.37 square kilometers and 1509.23 square kilometers, respectively, for a total of 2403.60 square kilometers. The average annual temperature in the watershed is 21.9 degrees Celsius, while it is 13 degrees Celsius in the mountains. This region is classified as having arid and semi-arid weather. The geographical location of the studied area is shown in Fig. 1.

2.2. Methodology

This study used two phases of spatial analysis and spatial statistics in ArcGIS Pro to accurately evaluate the hazard of flooding in the studied area. The general steps in the first phase (spatial analysis) include data collection, rasterization, standardization using fuzzy membership functions, weighting by employing the hierarchical method, and overlaying the layers using fuzzy operators. After preparing the flood hazard zone, kernel density and zonal statistics were used for calculating the flooding hazard density based on the distribution of residential areas and zoning the flooding hazard based on land cover. Furthermore, spatial statistics (the second phase) in ArcGIS Pro were used to find the high and low-risk areas of flooding. In this phase, the spatial distribution pattern of flooding in the studied area was identified globally by using spatial autocorrelation and average nearest neighbor; high-risk and low-risk clusters of flooding were identified locally using hot spot analysis and cluster and outlier analysis.

2.2.1 Spatial analysis

Flood hazard mapping

According to the literature (Mngutyo et al., 2013; Ogato et al., 2020; Kazakis et al., 2015), seven criteria, including height, slope, drainage density, NDVI, land cover, geology, and precipitation were selected as the

effective criteria of flooding hazard in the studied area. These characteristics correspond to the Environmental Protection Agency's and Interior Ministry's standards and requirements, as well as global experience (Table 2). In this research, flooding hazard zoning was executed in four phases, the most critical of which were fuzzification and weighing the criteria.

Table 2
Characteristics of the effective criteria in flood hazard mapping

Data	Format-type	Accuracy (meter)	Source
Drainage density	Vector-line	12.5	DEM
Geology	Vector-polygon	25000	Geological Survey of Iran
Slope	Raster	12.5	DEM
DEM	Raster	12.5	Vertex.daac.asf.alaska.edu
Land cover	Vector-polygon	500	General Department of Natural Resources of Fars province, Iran
Precipitation	Vector-line	250	Iran Meteorological Organization
NDVI	Raster	30	https://earthexplorer.usgs.gov/

Rasterization

The input information should have a raster structure for fuzzifying the layers. Therefore, in this study, all the information layers prepared (excluding DEM and Slope) in ArcGIS Pro were rasterizied using different tools, including raster calculator, feature to raster, interpolation, and kernel density. In this step, the cell size of all the layers was determined based on the size of DEM layer.

Fuzzification or standardization

The Iranian scientist Lotfi Zadeh presented the Fuzzy Logic Theory for the first time for acting in conditions of uncertainty. For membership, Or, And, Product, Sum, and Gamma are the basic strengths of this integration model. This method used in this study is one of the most practical integration models in various sciences, such as environmental planning (Yager et al., 2012). One of the most fundamental issues in fuzzy theory is the discussion of the membership function and how it is defined. The basic difference between fuzzy and other methods is the definition of the membership function. The membership function can be defined as the degree of belonging to the elements of the reference set to its subsets and is represented as μc (X).

In this step, the raster layers of each of the factors affecting the flooding hazard in the Darab watershed are converted to the fuzzy layers by using membership functions including Sigmoidal, Linear, and User defined in ArcGIS Pro and Terrset software and in the Python programming environment (Table 3).

Table 3
Standardization of the criteria based on the fuzzy membership functions

Main Criteria	Fuzzy Function	Control points
NDVI	Linear (decreasing)	a=-0.17 b = 0.1
Land cover	User defined	Poor land = 0.8, moderate land = 0.6, agriculture and garden = 0.3 urban = 0.4 without cover = 0.9 forest = 0.15
Dem	Sigmoidal (increasing)	a = 1025 b = 2500
Slope	Sigmoidal (increasing)	a = 5 b = 20
Drainage Density	Sigmoidal (decreasing)	a = 0.1 b = 0.6
Rain	Linear (increasing)	a = 100 b = 260
Geology	User defined	The geological formations used in this area are as follows: 1. Salt Domes (Hormoz Series) 2. Kozhdami Formation 3. Sarvak Formation 4. Tarbour Formation 5. Sachun Formation 6. Asmari Formation of Jahrom 7. Fars Group Formations (Gachsaran Formation, Mishan Formation and Aghajari Formation) 8. Bakhtiari Formation 9. New alluvium. The Asmari-Jahrom Formation, which is composed of lime and dolomite, is widely exposed in southern Iran. Asmari-Jahrom is enclosed between the impermeable formations of Razak or Gachsaran and the Pabdeh Gurpi and Sachun formations. The salt dome, Sarvak, Bakhtiari, New Alluvium, Tarbour, and Aghajari formations have high permeability, and the Gozhdmi and Mishan formations have low permeability.

In the next step, these layers can be overlayed by utilizing fuzzy operators after fuzzifying the rasterizied layers. The problem associated with these fuzzification layers in overlaying was that they had the same importance and weight as all the layers, given that a criterion such as drainage density was more important than the NDVI criterion. This problem was solved using the Analytical Hierarchy Process. Therefore, each of the fuzzification layers has value and importance. These values were scored based on the judgment of the specialists and experts on seven criteria.

Weighting the criteria by AHP

Prioritizing the criteria and sub-criteria

This study used the multi-criteria analysis method based on GIS to prioritize or weight the criteria for identifying areas with a flood hazard (Wang et al., 2011; Zou et al., 2013; Gigovi´c et al., 2017; Rimba et al., 2017). The Analytical Hierarchy Process (AHP) is one of the multi-criteria decision-making systems for zoning the hazard of flooding, which is widely used. AHP plays an important role in valuing the various factors in zoning the hazard of flooding (Ogato et al., 2020). In this study, weighting seven standardized criteria for determining the area with a high hazard of flooding is the main purpose of using the Analytical

Hierarchy Process in GIS. The specialist from different departments including environment, natural resources, agriculture, municipality, as well as the experts, social activists and beneficiaries were used for weighting. Firstly, the weight of criteria and sub-criteria was determined by using the judgment of local experts. The AHP method is performed in four main steps (Bathrellos et al., 2012; Yang et al., 2013; Ouma and Tateishi, 2014).

The first step involves analyzing the decision-making problem in a hierarchical structure in which goals, criteria, and sub-criteria are determined. The next step in the AHP method is based on the pairwise comparisons used for determining the weights for different criteria. The weight of a particular criterion is determined by ranking its importance and appropriateness. Evaluating the pairwise comparisons is conducted by the judgment of the experts (Saaty, 1977). The importance and preference in the pairwise comparisons were determined by using a scale of 1–9 hours (Table 4).

Table 4
Pairwise comparison scale in AHP (Saaty and Vargas, 2001)

Intensity of importance	Definition	Explanation
1	Equal importance	Two attributes preferred equally
2	Weak or slight	Judgement indicates weak favoring of one attribute over another
3	Moderate importance	Judgement slightly favored one element over another
4	Moderate plus	Judgement moderately favored one element over another
5	Strong importance	Judgement strongly favored one element over another
6	Strong plus	Judgement slightly more than strongly favored one element over another
7	Very strong or demonstrated importance	Judgement very strongly favored one element over another
8	Very, very strong	Judgement very, very strongly favored one element over another
9	Extreme importance	Extreme preference of one attribute over the another

The third step is calculating the final weight of each criterion based on the conducted pairwise comparisons. In AHP, C = {Cj | j = 1,2,…, n} shows the set of criteria. In this set, the result of a pairwise comparison of n criteria can be summarized in (n_n). Each element aij (i, j = 1,2,.., n) in the matrix A finally created the total weight of each parameter in this study. Matrix A is shown in Eq. 1 (Ouma and Tateishi, 2014).

$$A = \begin{bmatrix} a_{11} & a_{12} & a_{1n} \\ a_{21} & a_{22} \cdot & a_{an} \\ . & . & . \\ a_{n1} & a_{n2} \cdot & a_{nn} \end{bmatrix}, a_{ii} = 1, a_{jj} = 1 / a_{jj}, a_{jj} \neq 0 \text{ (Eq. 1)}$$

Assessing the consistency ratio was the last step. Inconsistencies may occur due to the intervention of an expert's judgment. This ratio indicates whether the comparisons are consistence or not. The consistency of the matrix is indicated when this rate is less than 0.1, and the pairwise comparisons should be reconsidered when it is more than 0.1. The consistency ratio is calculated based on Eq. 2. In this study, the weighting steps were conducted using AHP in Excel.

CR = CI / RI (Eq. 2)

This equation shows the consistency index (CI), which is calculated using Eq. 3.

CI = (λmax - n) / (n − 1) (Eq. 3)

λmax in this equation is considered as the sum of each column in the pairwise comparison matrix and the weight of each. Moreover, n shows the size of the matrix, which is equal to the number of criteria. The Random index (RI) indicates the chance of a consistency rate of the pairwise comparison matrix judged by specialists, calculated by the hour per matrix size (n) (Table 5). In this study, RI was equal to 1.32 for seven parameters. CR indicates the consistency ratio.

Table 5
Random index (RI) used for computing the consistency ratios (CR) (Saaty, 1977)

n	1	2	3	4	5	6	7	8	9	10
R1	0.00	0.00	0.58	0.90	1.12	1.24	1.32	1.41	1.45	1.49

Overlaying layers using the fuzzy logic operators

Fuzzy overlaying

In the fuzzy method, classes and spatial units with membership degrees of 0–1 can be defined for each raster layer. Then, each fuzzification layer was combined with each other by using fuzzy operators. These operators include Or, And, Sum, Product, and Gamma. This is performed in ArcGIS Pro by using the fuzzy overlay tool available in the spatial analysis toolbox. All the standardized and weighted layers with all the operators were overlaid in turn by using the tool. In this study, the cell size of the layers was considered to be 12.5 meters based on the cell size of the layer of the Digital Elevation Model (DEM). Further, the coordinate system of all the layers was in zone 40 based on the UTM and Datum WGS84 projection systems.

Kernel density

This study used kernel density in order to calculate the density of flooding hazard in residential areas in the Darab watershed. First, the pixel value of the final layer of the flood hazard for 302 residential areas was entered into the descriptive table of the point layer of residential areas by using the extract values to point tool, and each point had a value or share of the flooding hazard. A symmetric region is created around each phenomenon in kernel density, and a value is calculated for each position within the symmetric region based on the distance from the point to the phenomenon. Therefore, kernel density is assumed to be a function of distance, and based on that, the required calculations are performed in the search radius (Silverman BW, 1986).

Zonal statistics

The zonal statistics technique computes data on the cell values included inside a raster. Zonal Statistics and Zonal Statistics as a Table are two methods for calculating statistics according to zones. The Zonal Statistics framework computes a single statistic at a time and outputs it as a raster. This value becomes the cell value for the cells associated with that zone in the raster output. If a zone feature has overlapping zones, the statistic is generated for just one zone, since each cell in the output raster may reflect only one value (Hyndman and Fan, 1996). Zonal statistics analysis, which is available in the spatial statistics toolbox in ArcGIS Pro was used for zoning the hazard of flooding based on land cover and land type. Based on the imported polygons or zones, this tool calculates the average and range of the value of raster layer cells (flooding hazard) based on the classification of polygons.

2.2.2 Spatial statistics

The analysis of spatial autocorrelation and the average nearest neighbor (global Moran) were performed to identify the high-risk and low-risk clusters of residential areas related to flooding after spatial analysis of flooding hazard. Identifying the high-risk and low-risk clusters of floods in the study area is conditional on the residential areas with flood hazard having a cluster spatial distribution pattern.

Average nearest neighbor

The average nearest neighbor calculation calculates the distance between the center of each feature and the central position of its nearest neighbor and then displays the average of these distances. The distribution pattern of features will be clustered and dispersed if the average distance is less and greater than the hypothetical random distribution, respectively. Moreover, the distribution pattern is clustered and random when the rate of the average nearest neighbor is less than or equal to 1, respectively.

Spatial autocorrelation

Spatial autocorrelation plays an important role in spatial modeling. The distribution pattern of flooding can be analyzed based on the created polygons by using the results of this test. The value of the Global Moran's Index is in the range of -1 to + 1. The distribution of flooding is clustered and random if the

Moran's index is greater than or lower than zero, respectively. Further, the distribution is dispersed if the index is equal to zero.

Hot spots analysis

Finally, hot spot analysis was used to assess the location of high-risk and low-risk clusters in the flooding areas. Hotspots analysis calculates the Getis-Ord Gi* statistic for all the residential areas in the study area. By this method, the hotspots, or places where residential areas are clustered, can be indicated by displaying the standard score values and the probability value.

Cluster and Outlier analysis

Like hot spot analysis, in addition to the high-risk and low-risk clusters, cluster and outlier analysis evaluates the location of outliers. Anselin local Moran's I divides the results (polygons) into five categories, which include high-high and low-low, indicating the cluster pattern, and high-low and low-high, showing the outlier pattern and not significant. High-high polygons indicate the areas with high-risk clusters or flooding hotspots. Low-low polygons show low-risk clusters or flooding cold spots (Peeters et al., 2015).

3. Results

After library studies and knowing the situation of the studied area, in the first step, all the input data as the effective criteria in the hazard of flooding converted to the raster layers in ArcGIS Pro using various tools. The raster layers of seven criteria, including dem, slope, drainage density, NDVI, land cover, geology, and precipitation are shown in Fig. 2. Only land cover and geology have polygon structure among the raster layers, which were rasterized using the feature to raster tool. The value of the raster cells increases from blue to red in other raster layers with the structure of a point or polyline rasterized using the Euclidean distance, interpolation tool and kernel density. In other words, the red cells (except geology and land cover) indicated the high values. Among these layers, drainage density and NDVI were inversely related to the hazard of flooding. However, precipitation, dem, and slope were directly associated with the hazard of flooding (Ogato et al., 2020; Argaz et al., 2019).

After rasterization of the criteria, the rasterized layers were standardized by using different fuzzy membership functions based on the library and field studies. The standardized layers have values between 0 and 1. The numbers in these layers that are close to 1 indicate a high risk of flooding (Fig. 3). It shows that the precipitation criterion in the Darab watershed's center, which has the most population, has a considerable proclivity to flood. Precipitation criteria such as slope, dem, land cover, NDVI, and geology had a low potential for flash floods at the survey boundary's center, with the greatest potential for flooding towards the study area's margin. The majority of the survey borders demonstrated a high desirability to flood risk in the fuzzy layer of drainage density. Table 6 indicates the final weight of each of the criteria selected in this study. The criteria of drainage density, slope, land cover, precipitation, geology, dem, and NDVI had the highest weights, respectively. Drainage density, slope, and land cover, with a final weight of 0.2737, 0.1716, and 0.1533, respectively, had the highest value among the criteria,

which had the greatest effect on overlaying the layers. In the fuzzification layer of drainage density, which is the most important among the variables, more pixels of the study area were introduced as the areas with the flood hazard compared to the other variables, excluding NDVI. Unlike in the slope layer, fewer pixels are at risk of flooding, which is mostly located in the northern regions of the study area.

Table 6
Significance weights of the main criteria and sub-criteria

Main criteria	W1	Sub-criteria	W2	Final Weight
Hydroclimate	0.411	Drainage Density	0.666	0.2737
		Rain	0.333	0.1368
Topography	0.261	Dem	0.333	0.0858
		Slope	0.666	0.1716
Land type	0.327	Land cover	0.475	0.1553
		Geology	0.415	0.1357
		NDVI	0.109	0.0356

The final layers obtained from overlaying by five fuzzy operators are shown in Fig. 4. The red and blue spots on the output maps were considered to be places with a high and low risk of flooding, respectively. Finally, the zonation of flooding potential was created by overlaying the weighted fuzzy layers by using different fuzzy operators, which is the best method for zoning the hazard of flooding based on the conducted studies (Mngutyo et al., 2013; Ogato et al., 2020; Kazakis et al., 2015). Other operators, except Or and Sum, which showed illogical results based on the flooding, indicated that the highest flood hazard is related to the north and south of the study area near the altitudes of the Darab watershed. Among these operators, the Gamma operator (0.9) showed the best and most logical result compared to the other operators, based on the value range of the cells.

Figure 5A indicates the total area of the regions with a high hazard of flooding is approximately 63432.7344 hectares, which contains pixels with a value above 0.5 and shows the red and orange spots. Moreover, the areas with moderate flood hazard (0.15–0.5) include 86204.2969 hectares of the Darab watershed. The highest area is related to the values less than 0.015, with a total area of 90131.8281 hectares, which shows the blue and safe spots on the map. As shown in Fig. 5B, the majority of the residential areas within the study area are in areas with a low to moderate hazard of flooding. The non-hazardous pixels were located at the left and right of the study area (Fig. 5A) and were removed from the next analysis of the study due to the absence of residential areas and lack of flooding in these regions. In Fig. 5A, areas with high, moderate, and low hazard include 63280.2188, 85809.4375, and 5909.7344 hectares of the secondary boundary, respectively. The georeferenced points were used for verifying the obtained results. These points were collected from the studied area using the GPS device and field visits from flooding areas under the supervision of the experts and locals during the rainy years (recent 10

years). Every 60 GPS points were converted to the ship file format in ArcGIS software and overlaid on the final zone of flooding hazard (Fig.5B).

Based on the results of the verification, most of the GPS points were located in areas with a high hazard of flooding. Each point indicates a significant and somewhat damaging flood in its surrounding areas. Based on the range of values of each zone (Fig. 4) and the ground truth map, the Gamma operator (0.9) was the best selection for the final zone of flooding hazard (Fig. 6).

In the study area, the total residential areas include 302 villages, most of which, especially the places showing the highest density on the map and considered the most populous areas, are probably located in moderate and low-hazard areas. To ensure this issue, the kernel density estimation tool was used to estimate the flood hazard density in residential areas after performing the kernel density estimation on residential areas (Fig. 7).

In Fig. 7, the darker blue pixels indicate the higher density of flood hazard in the study area. In other words, the dark blue spots in the Darab watershed, which are mostly located in the center of the boundary, show a high hazard of flooding in residential areas. However, it cannot be certainly said that high-hazard residential areas are located in the center of the study area since, in addition to the weight (flood hazard) of residential points, kernel density estimation considers the location of points and their distance from each other for estimating the density. Therefore, global and local Moran analysis was used in the next steps to further ensure. As shown in Fig. 8A, the spatial distribution pattern of unweighted population points is clustered.

In this analysis, the nearest neighbor ratio is above zero (0.607) and P-value is equal to zero, which indicates that the spatial distribution pattern of unweighted residential points, i.e., the spatial distribution pattern was evaluated only based on the location of points and their distance from each other, is significant and clustered (Z-score is equal to -13.05). Moreover, in Fig. 8B, the distribution pattern of weighted residential areas with flooding hazard is clustered. Based on the results indicating the highest degree of significance (P-value = 0), Moran's index is above zero (Moran's index = 0.359) and the Z-score is equal to 10.95, showing the spatial distribution pattern of the weighted residential areas is clustered.

Hotspots analysis (local Moran) was used to identify the high-risk and low-risk clusters after ensuring the clustering of the distribution pattern of residential areas (unweighted and weighted). After performing hotspot analysis on the weighted residential areas with flooding hazards, Fig. 9A was obtained, which indicates three categories of low-risk clusters or cold spots with a confidence level of 90, 95, and 99%, which are shown in blue. Three categories of high-risk clusters or hotspots with a confidence level of 90, 95, and 99% exist in this figure, which are indicated in red. Furthermore, there is a category without a confidence level, which is displayed in gray and smaller spots. Low-risk clusters of residential areas relative to flooding with a 99% confidence level are located in the west and east of the study area (blue). However, high-risk clusters of flooding with a 99% confidence level are dispersed in the north and northeast (red) of the study area at higher altitudes. The other points are not statistically significant and do not show a reliable result.

Cluster and outlier analysis were used to identify the high-risk and low-risk clusters of residential areas more accurately. In Fig. 9B, two categories, including High-High and Low-Low clusters, indicated the high-risk and low-risk clusters, respectively, whose distribution is similar to the output of hotspot analysis. Moreover, two categories, including High-Low outlier and Low-High outlier, show the outliers. The first category indicates that high-hazard residential areas were surrounded by low-hazard residential areas that were flooded. However, no residential properties with these characteristics were observed in this study. The second category (Low-High outlier) shows the residential areas with low flood potential around which high flood hazard residential areas are located. Such residential areas can be considered areas at high flood risk due to their proximity to areas with a high hazard of flooding. In this study, a residential point called Fatah al-Mubin town is located in this category. Therefore, the residential clusters in the north and northeast of the watershed (with a population of less than 5000 people) are at risk of flooding. In this regard, necessary measures should be taken by managers, environmental planners, and municipalities.

Two effective indices on the output of this analysis, including Z-score and P-value, were categorized using Symbology for assessing the results of the hotspot analysis in more detail. In Fig.10A, the points with Z-score higher than 2.5 and lower than − 2.5 indicate the high-risk clusters and low-risk clusters of hotspot analysis with 99% confidence. The P-value shows the significance of the identified clusters. The confidence level of clusters decreased when the distance from 0 to 1 was increased. As shown in Fig. 10B , blue points indicate the high-risk and low-risk clusters of flooding with a 99% confidence level.

Figure 10. Hotspot analysis of flooding areas, A: Z-score, B: P-value

Land cover is a key factor in the occurrence of floods. Precipitation in the land without vegetation flows quickly on the ground compared to forest areas. Therefore, severe runoff flows in some land areas (for instance, a high percentage of urban) compared to the similar areas covered by forest and grass (Bakhtyari Kia 2012). 14 Land cover variable, indicating the type of land (man-made or natural) for a specific application such as urban, agricultural, industrial, rangeland, and forest, is one of the most important factors affected by the flood hazard. The map of flooding obtained by overlaying fuzzy operators was zoned in the studied area (Fig. 11).

After applying the Zonal Statistics analysis in this zoning, the maximum rate of flooding hazard exists in poor and moderate grassland covers (blue polygons), which are located in the marginal areas of the study area. Moreover, the minimum level of hazard of flooding was observed in the urban, agricultural, forest, and garden uses (yellow, orange, and red polygons) in the boundary center and near the populous centers of the Darab watershed.

4. Discussion

Multiple techniques are available for calculating runoff and surveying the actual flash flood risk. The majority of techniques are graphical in nature and include the use of empirical equations, statistical

evaluation of flood data, which is the subdivision of flood data into a number of sub-basins, remotely sensed data, and GIS (Tehrany, 2013). The flooding risk was assessed using spatial analysis and spatial statistics techniques in GIS. Previous studies implemented a set of criteria to pinpoint flood threats. Dano et al. (2019) evaluated the flood danger in the Perlis basin, Malaysia, by integrating various layers of land cover, residential areas, structural geology, and precipitation. Ogato et al. (2020) employed a number of separate layers to describe flooding potential hazard, comprising land use / land cover, altitude, slope, drainage density, subsoil, and rainfall. Additionally, Kabir and Mir (2021) assessed the feasibility of shelter in Bangladesh's flooding zones using elements such as dem, land cover, landform, population density, accessibility, distance to roadway, and distance to town.

The present investigation utilized layers comprising slope, dem, geomorphology, land cover, NDVI, precipitation, and drainage density for spatial and statistical analysis of floods. The membership level was then calculated, and the model was examined for each of the layers based on their relationship to the flood risk as defined by the fuzzy operations. According to the findings of this research, the fuzzy model is sophisticated, however it also offers significant advantages for analyzing diverse phenomena associated with the earth's surface. Moreover, according to the final map produced using fuzzy logic and AHP, zones with a very high risk of flooding are located in the northern and northeast regions of the surveyed area, which covers 63432.7344 hectares of the Darab watershed's total area. Low hazard areas are often located in plains, valleys, and thalwegs, which have lower slopes. Additionally, the Gamma operator (0.9) was determined to be the optimal fuzzy overlay operator. Shariati et al. (2020) used ArcGIS's geographical analysis and spatial statistics frameworks effectively in a spatial scientific investigation. Significant spatial statistical components, such as the detection of high-risk and low-risk clusters, were applied to zone flood danger in this analysis, which differentiates this research from previous studies (Mngutyo et al., 2013; Ogato et al., 2020; Argaz et al., 2019; Kazakis et al., 2015; Ouma et al., 2014).

The current study verified the cold and hot points of flooding with a 95% confidence level. The highest at-risk clusters of floods are positioned in the north and northeast parts of the experiment boundaries, near the heights linked to villages with less than 5000 inhabitants. Furthermore, the increase in risk does not pose a threat to man-made uses such as suburban buildings, farmlands, and gardens. Nevertheless, the risk of flooding has been detected, particularly in the north of the study boundaries, as a result of changes in the landscape toward the destruction of natural ecosystems by growing urbanization. Administrators should execute the appropriate planning. According to the observations, clusters and outliers' analyses, as well as hotspots analyses, are critical tools to recognize high and low-risk clusters (Shariati et al., 2020). This research found that integrating spatial analysis with spatial statistics is a valid and reliable tool for addressing phenomena like floods. Additionally, this approach can be applied in other analyses, such as mapping seismic vulnerability, karst development, and disease prevalence studies.

5. Conclusion

The criteria utilized in this study were valid and acceptable in light of previous research as well as knowledge of the survey's boundaries. Among the factors, drainage density, slope, precipitation, geology, dem, and NDVI have a final weight of 0.2737, 0.1716, and 0.1533, respectively, in the Darab watershed's flood risk zoning. Focusing on the verification and practical assessment findings as well as the range of values in the zoning layer, the Gamma operator (0.9) was considered as the optimum fuzzy logic overlay operator for flood hazard mapping. The survey boundary's most flood-prone locations were located far from heavily populated areas. However, there is a significant and extremely significant danger of flooding in several residential districts to the north and northeast of the study zone, which have fewer than 5000 inhabitants and comprise 363432.7344 hectares of the entire Darab watershed. Moreover, the greatest incidence of flooding danger was detected in the marginal areas of the study area in the poor and moderate range of usage. The lowest rate of flooding risk was reported in uses including urban, agricultural, forestry, and gardens situated in the Darab watershed's border center and near heavily inhabited areas.

The results of the verification using GPS points revealed that the majority of survey locations are situated in regions with a high risk of flooding. Each point shows the presence of a substantial and relatively destructive flood in the region immediately around it, confirming the veracity of the present research. Spatial statistics combined with spatial analysis may offer a robust technique for flooding studies since distinguishing between high-risk and low-risk clusters provides more accurate and confident findings for flooding danger associated with the distribution of residential areas. According to the results, kernel density estimation cannot be utilized independently to identify flood-prone clusters. As a result, the use of global and local Moran analysis is advantageous in this domain. In this study, Moran's index was shown to be 0.359 in the cluster distribution pattern, and high- and low-risk flood clusters can be recognized with a high level of confidence (P-value = 0). The combination of the two clusters, outlier analyses, and hotspot assessment is more effective in detecting high- and low-risk flooding clusters.

Declarations

Funding

The present work received no external financial support.

Acknowledgment

The authors would like to express their gratitude to the Geological Survey of Iran, the Fars province's General Department of Natural Resources, and the Meteorological Organization for providing research facilities.

Conflict of interests

The authors declare there is no conflict of interests that would influence this work.

References

1. Arabameri, A., Rezaei, K., Cerdà, A., Conoscenti, C., & Kalantari, Z (2019). A comparison of statistical methods and multi-criteria decision making to map flood hazard susceptibility in Northern Iran. *Science of The Total Environment, 660*, 443-458. https://doi.org/10.1016/j.scitotenv.2019.01.021
2. Argaz, A., Ouahman, B., Darkaoui, A., Bikhtar, H., Ayouch, E., & Lazaar, R (2019). *Flood Hazard Mapping Using remote sensing and GIS Tools: A case study of Souss Watershed*.
3. Bathrellos, G. D., Gaki-Papanastassiou, K., Skilodimou, H. D., Papanastassiou, D., & Chousianitis, K. G (2012). Potential suitability for urban planning and industry development using natural hazard maps and geological–geomorphological parameters. *Environmental Earth Sciences, 66*(2), 537-548. https://doi.org/10.1007/s12665-011-1263-x
4. Dano, U. L., Balogun, A.-L., Matori, A.-N., Wan Yusouf, K., Abubakar, I. R., Said Mohamed, M. A., . . . Pradhan, B (2019). Flood Susceptibility Mapping Using GIS-Based Analytic Network Process: A Case Study of Perlis, Malaysia. *Water, 11*(3). https://doi.org/10.3390/w11030615
5. Demir, V., & Kisi, O (2016). Flood Hazard Mapping by Using Geographic Information System and Hydraulic Model: Mert River, Samsun, Turkey. *Advances in Meteorology, 2016*, 4891015. https://doi.org/10.1155/2016/4891015
6. Desalegn, H., & Mulu, A (2021). Flood vulnerability assessment using GIS at Fetam watershed, upper Abbay basin, Ethiopia. *Heliyon, 7*(1). https://doi.org/10.1016/j.heliyon.2020.e05865
7. Feng, B., Zhang, Y., & Bourke, R (2021). Urbanization impacts on flood risks based on urban growth data and coupled flood models. *Natural Hazards, 106*(1), 613-627. https://doi.org/10.1007/s11069-020-04480-0
8. Ghazavi, R., Vali, A. B., & Eslamian, S (2012). Impact of Flood Spreading on Groundwater Level Variation and Groundwater Quality in an Arid Environment. *Water Resources Management, 26*(6), 1651-1663. https://doi.org/10.1007/s11269-012-9977-4
9. Gigović, L., Pamučar, D., Bajić, Z., & Drobnjak, S (2017). Application of GIS-Interval Rough AHP Methodology for Flood Hazard Mapping in Urban Areas. *Water, 9*(6). https://doi.org/10.3390/w9060360
10. Hyndman, R. J., & Fan, Y. (1996). Sample Quantiles in Statistical Packages. *The American Statistician, 50*(4), 361-365. https://doi.org/10.1080/00031305.1996.10473566
11. Kazakis, N., Kougias, I., & Patsialis, T (2015). Assessment of flood hazard areas at a regional scale using an index-based approach and Analytical Hierarchy Process: Application in Rhodope–Evros region, Greece. *Science of The Total Environment, 538*, 555-563. https://doi.org/10.1016/j.scitotenv.2015.08.055
12. Khoirunisa, N., Ku, C.-Y., & Liu, C.-Y (2021). A GIS-Based Artificial Neural Network Model for Flood Susceptibility Assessment. *International Journal of Environmental Research and Public Health, 18*(3). https://doi.org/10.3390/ijerph18031072

13. Kia, M. B., Pirasteh, S., Pradhan, B., Mahmud, A. R., Sulaiman, W. N. A., & Moradi, A (2012). An artificial neural network model for flood simulation using GIS: Johor River Basin, Malaysia. *Environmental Earth Sciences, 67*(1), 251-264. https://doi.org/10.1007/s12665-011-1504-z
14. Liu, Y., Lu, X., Yao, Y., Wang, N., Guo, Y., Ji, C., & Xu, J (2021). Mapping the risk zoning of storm flood disaster based on heterogeneous data and a machine learning algorithm in Xinjiang, China. *Journal of Flood Risk Management, 14*(1), e12671. https://doi.org/10.1111/jfr3.12671
15. Maryanaji, Z., Merrikhpour, H., & Vejdani Nozar, A (2020). Flood risk zoning based on the hydro-climatic characteristics of basins in Hamedan Province, Iran. *Journal of Advances in Environmental Health Research, 8*(2), 111-123. https://doi.org/10.22102/jaehr.2020.156067.1112
16. Mngutyo, I. D., & Ogwuche, J. A (2013). *URBAN DEVELOPMENT, FLOOD AND DISASTER MANAGEMENT: CHALLENGES OF CONTEMPORARY URBAN PLANNING PERSPECTIVES*. https://doi.org/10.4172/2324-9315.1000113
17. Modarres, R., Sarhadi, A., & Burn, D. H (2016). Changes of extreme drought and flood events in Iran. *Global and Planetary Change, 144*, 67-81. https://doi.org/10.1016/j.gloplacha.2016.07.008
18. Msabi, M. M., & Makonyo, M (2021). Flood susceptibility mapping using GIS and multi-criteria decision analysis: A case of Dodoma region, central Tanzania. *Remote Sensing Applications: Society and Environment, 21*, 100445. https://doi.org/10.1016/j.rsase.2020.100445
19. Norouzi, G., & Taslimi, M (2012). The Impact of Flood Damages on Production of Iran's Agricultural Sector. *12*, 921-926. https://doi.org/10.5829/idosi.mejsr.2012.12.7.1783
20. Ogato, G. S., Bantider, A., Abebe, K., & Geneletti, D (2020). Geographic information system (GIS)-Based multicriteria analysis of flooding hazard and risk in Ambo Town and its watershed, West shoa zone, oromia regional State, Ethiopia. *Journal of Hydrology: Regional Studies, 27*, 100659. https://doi.org/10.1016/j.ejrh.2019.100659
21. Osei, B. K., Ahenkorah, I., Ewusi, A., & Fiadonu, E. B (2021). Assessment of flood prone zones in the Tarkwa mining area of Ghana using a GIS-based approach. *Environmental Challenges, 3*, 100028. https://doi.org/10.1016/j.envc.2021.100028
22. Ouma, Y. O., & Tateishi, R (2014). Urban Flood Vulnerability and Risk Mapping Using Integrated Multi-Parametric AHP and GIS: Methodological Overview and Case Study Assessment. *Water, 6*(6). https://doi.org/10.3390/w6061515
23. Park, K., & Won, J.-h (2019). Analysis on distribution characteristics of building use with risk zone classification based on urban flood risk assessment. *International Journal of Disaster Risk Reduction, 38*, 101192. https://doi.org/10.1016/j.ijdrr.2019.101192
24. Peeters, A., Zude, M., Käthner, J., Ünlü, M., Kanber, R., Hetzroni, A., . . . Ben-Gal, A (2015). Getis–Ord's hot- and cold-spot statistics as a basis for multivariate spatial clustering of orchard tree data. *Computers and Electronics in Agriculture, 111*, 140-150. https://doi.org/10.1016/j.compag.2014.12.011
25. Pham, B. T., Luu, C., Phong, T. V., Nguyen, H. D., Le, H. V., Tran, T. Q., . . . Prakash, I (2021). Flood risk assessment using hybrid artificial intelligence models integrated with multi-criteria decision analysis

in Quang Nam Province, Vietnam. *Journal of Hydrology, 592*, 125815. https://doi.org/10.1016/j.jhydrol.2020.125815

26. Pourghasemi, H. R., Razavi-Termeh, S. V., Kariminejad, N., Hong, H., & Chen, W (2020). An assessment of metaheuristic approaches for flood assessment. *Journal of Hydrology, 582*, 124536. https://doi.org/10.1016/j.jhydrol.2019.124536
27. Psomiadis, E., Tomanis, L., Kavvadias, A., Soulis, K. X., Charizopoulos, N., & Michas, S (2021). Potential Dam Breach Analysis and Flood Wave Risk Assessment Using HEC-RAS and Remote Sensing Data: A Multicriteria Approach. *Water, 13*(3). https://doi.org/10.3390/w13030364
28. Rahmati, O., Zeinivand, H., & Besharat, M (2016). Flood hazard zoning in Yasooj region, Iran, using GIS and multi-criteria decision analysis. *Geomatics, Natural Hazards and Risk, 7*(3), 1000-1017. https://doi.org/10.1080/19475705.2015.1045043
29. Rimba, A. B., Setiawati, M. D., Sambah, A. B., & Miura, F (2017). Physical Flood Vulnerability Mapping Applying Geospatial Techniques in Okazaki City, Aichi Prefecture, Japan. *Urban Science, 1*(1). https://doi.org/10.3390/urbansci1010007
30. Rincón, D., Khan, U. T., & Armenakis, C (2018). Flood Risk Mapping Using GIS and Multi-Criteria Analysis: A Greater Toronto Area Case Study. *Geosciences, 8*(8). https://doi.org/10.3390/geosciences8080275
31. Saaty, T. L (1977). A scaling method for priorities in hierarchical structures. *Journal of Mathematical Psychology, 15*(3), 234-281. https://doi.org/10.1016/0022-2496(77)90033-5
32. Saaty, T., & Vargas, L. (2001). *Models, Methods, Concepts & Applications of the Analytic Hierarchy Process*. https://link.springer.com/book/10.1007/978-1-4615-1665-1
33. Saha, A., Pal, S. C., Arabameri, A., Blaschke, T., Panahi, S., Chowdhuri, I., . . . Arora, A (2021). Flood Susceptibility Assessment Using Novel Ensemble of Hyperpipes and Support Vector Regression Algorithms. *Water, 13*(2). https://doi.org/10.3390/w13020241
34. Shariati, M., Mesgari, T., Kasraee, M., & Jahangiri-rad, M (2020). Spatiotemporal analysis and hotspots detection of COVID-19 using geographic information system (March and April, 2020). *Journal of Environmental Health Science and Engineering, 18*(2), 1499-1507. https://doi.org/10.1007/s40201-020-00565-x
35. Silverman, B. W. (2018). *Density estimation for statistics and data analysis*: Routledge. https://doi.org/10.1201/9781315140919
36. Svetlana, D., Radovan, D., & Ján, D (2015). The Economic Impact of Floods and their Importance in Different Regions of the World with Emphasis on Europe. *Procedia Economics and Finance, 34*, 649-655. https://doi.org/10.1016/S2212-5671(15)01681-0
37. Tang, J., Li, Y., Cui, S., Xu, L., Hu, Y., Ding, S., & Nitivattananon, V (2021). Analyzing the spatiotemporal dynamics of flood risk and its driving factors in a coastal watershed of southeastern China. *Ecological Indicators, 121*, 107134. https://doi.org/10.1016/j.ecolind.2020.107134
38. Tanoue, M., Hirabayashi, Y., & Ikeuchi, H (2016). Global-scale river flood vulnerability in the last 50 years. *Scientific Reports, 6*(1), 36021. https://doi.org/10.1038/srep36021

39. Tehrany, M. S., Pradhan, B., & Jebur, M. N (2013). Spatial prediction of flood susceptible areas using rule based decision tree (DT) and a novel ensemble bivariate and multivariate statistical models in GIS. *Journal of Hydrology, 504*, 69-79. https://doi.org/10.1016/j.jhydrol.2013.09.034
40. Uddin, K., & Matin, M. A (2021). Potential flood hazard zonation and flood shelter suitability mapping for disaster risk mitigation in Bangladesh using geospatial technology. *Progress in Disaster Science, 11*, 100185. https://doi.org/10.1016/j.pdisas.2021.100185
41. UNISDR & CRED (2018). Economic Losses, Poverty & Disasters (1998-2017). Available online at https://www.cred.be/unisdr-and-cred-report-economic-losses-poverty-disasters-1998-2017
42. Wang, Y., Li, Z., Tang, Z., & Zeng, G (2011). A GIS-Based Spatial Multi-Criteria Approach for Flood Risk Assessment in the Dongting Lake Region, Hunan, Central China. *Water Resources Management, 25*(13), 3465-3484. https://doi.org/10.1007/s11269-011-9866-2
43. WHO (2019). Iran floods leave people with limited access to life-saving health services. Accessed date: 13 May 2019. Available online at http://www.emro.who.int/eha/news/iran-floods-leave-people-with-limited-access-to-life-saving-health-services.html
44. WHO (2021). An overview on floods. Accessed date: 15 February 2021. Available online at https://www.who.int/health-topics/floods#tab=tab_1
45. Yager, R. R., & Zadeh, L. A (2012). *An introduction to fuzzy logic applications in intelligent systems* (Vol. 165): Springer Science & Business Media. https://link.springer.com/book/10.1007/978-1-4615-3640-6
46. Yang, X.-l., Ding, J.-h., & Hou, H (2013). Application of a triangular fuzzy AHP approach for flood risk evaluation and response measures analysis. *Natural Hazards, 68*(2), 657-674. https://doi.org/10.1007/s11069-013-0642-x
47. Zadeh, L. A. (1988). Fuzzy logic. *Computer, 21*(4), 83-93. https://doi.org/10.1109/2.53
48. Zou, Q., Zhou, J., Zhou, C., Song, L., & Guo, J (2013). Comprehensive flood risk assessment based on set pair analysis-variable fuzzy sets model and fuzzy AHP. *Stochastic Environmental Research and Risk Assessment, 27*(2), 525-546. https://doi.org/10.1007/s00477-012-0598-5

Tables

Table 1 is not available with this version

Figures

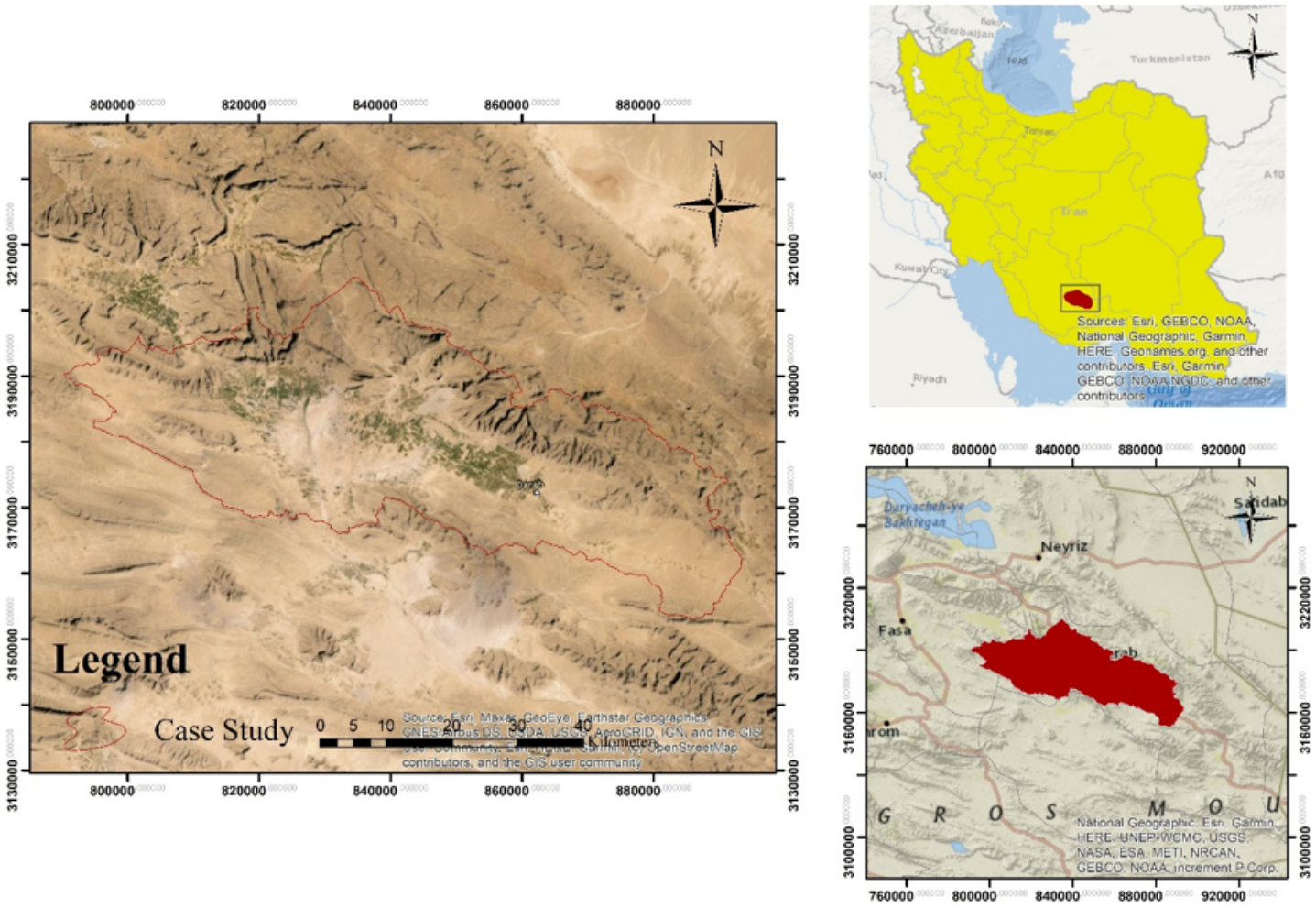

Figure 1

Geographical location of the Darab watershed

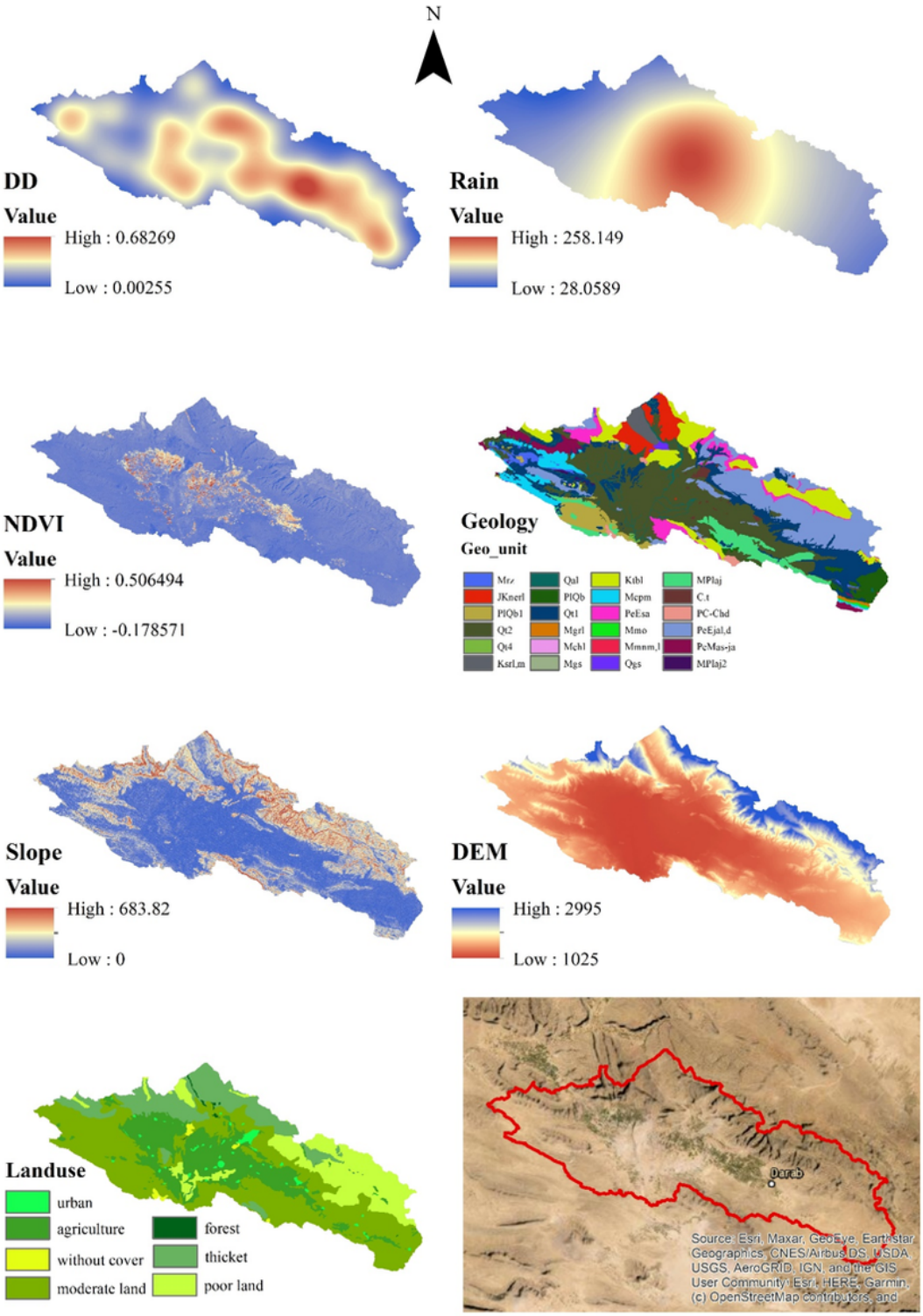

Figure 2

Criteria map of dem, slope, drainage density, NDVI, land cover, geology, and precipitation

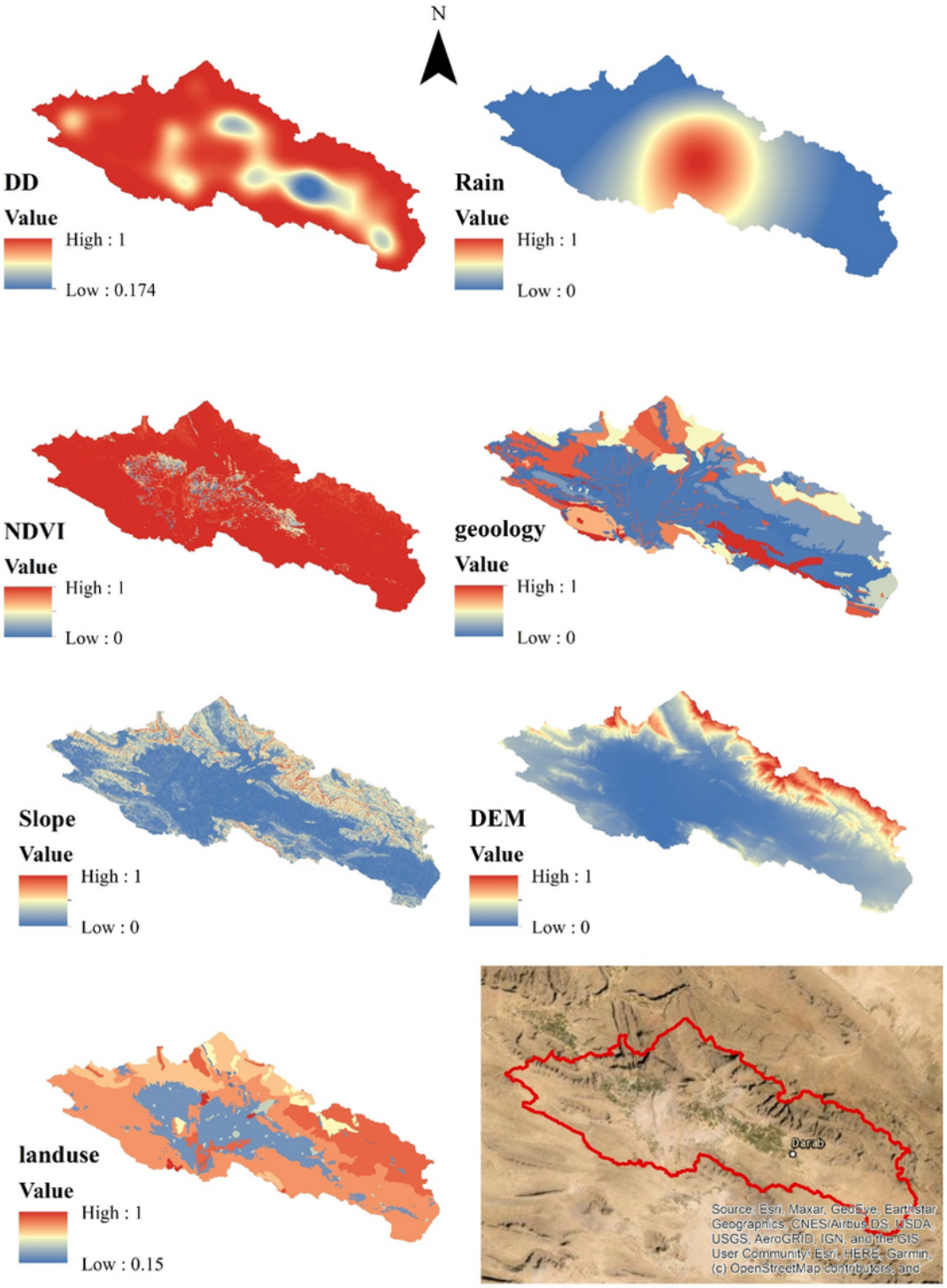

Figure 3

Fuzzification maps of dem, slope, drainage density, NDVI, Land cover, geology, and precipitation criteria

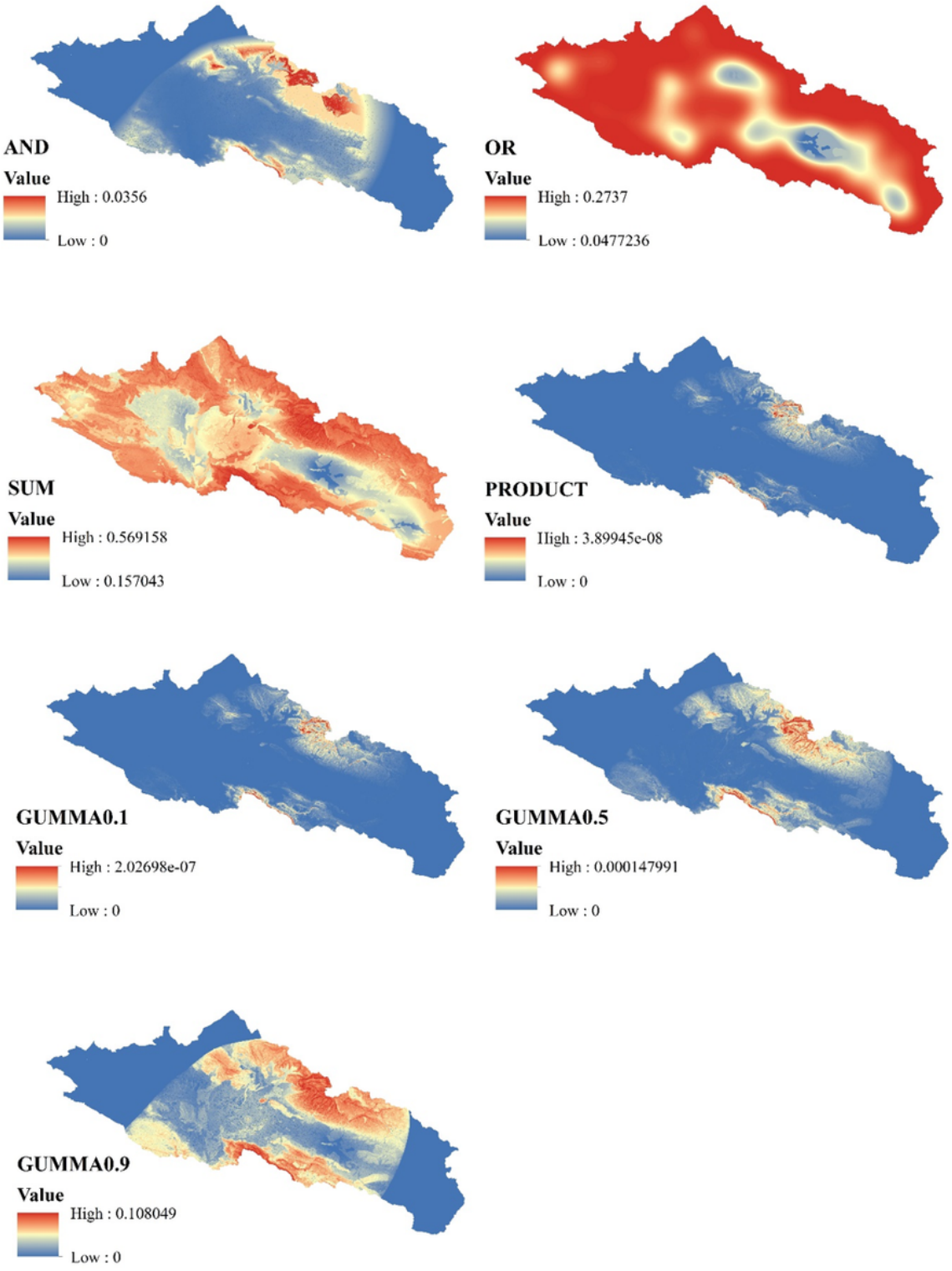

Figure 4

The obtained maps by overlaying the weighted fuzzy layers using fuzzy operators including AND, Or, Sum, Product, Gumma 0.9, Gamma 0.5, Gamma 0.1

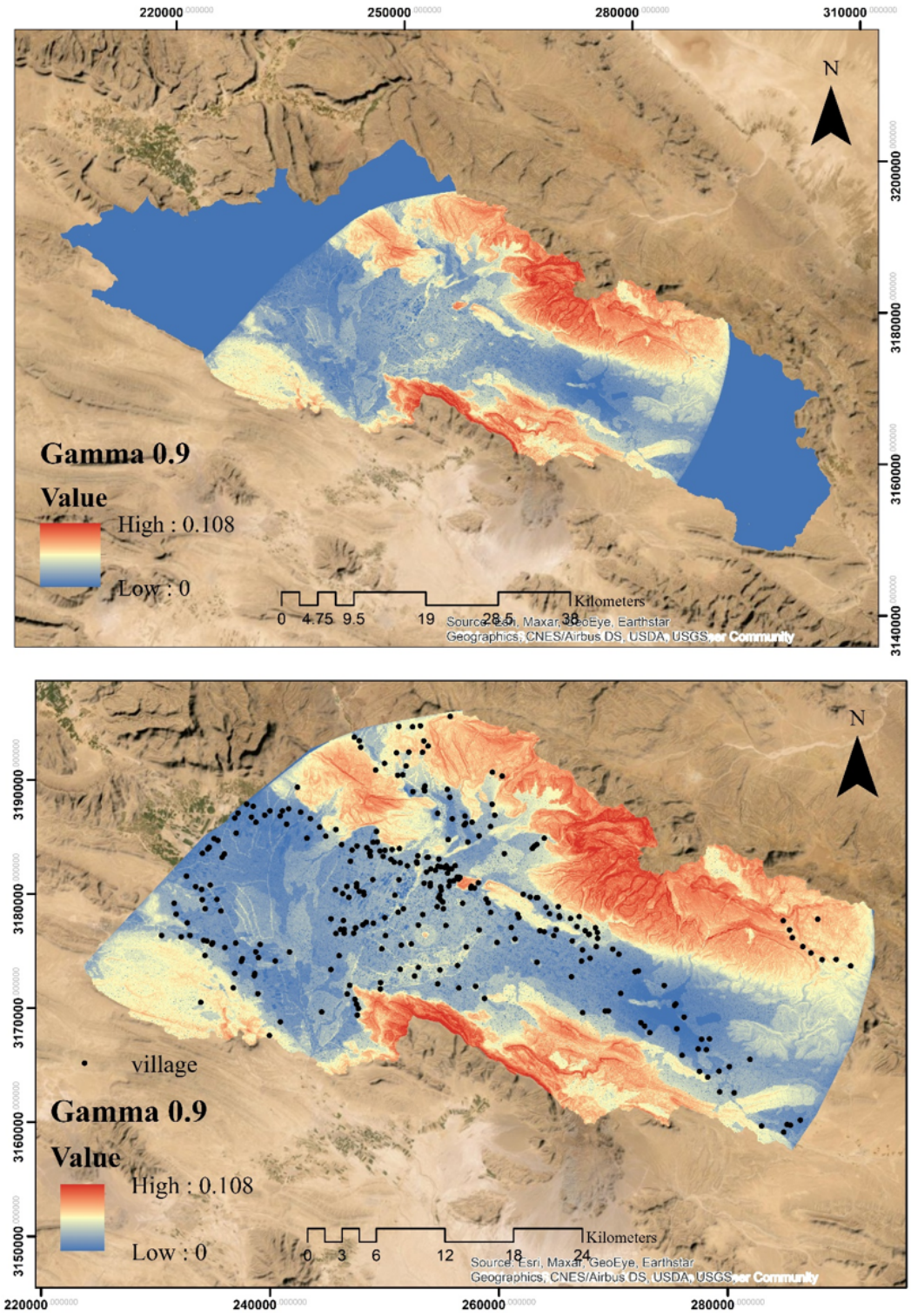

Figure 5

Flood hazard mapping

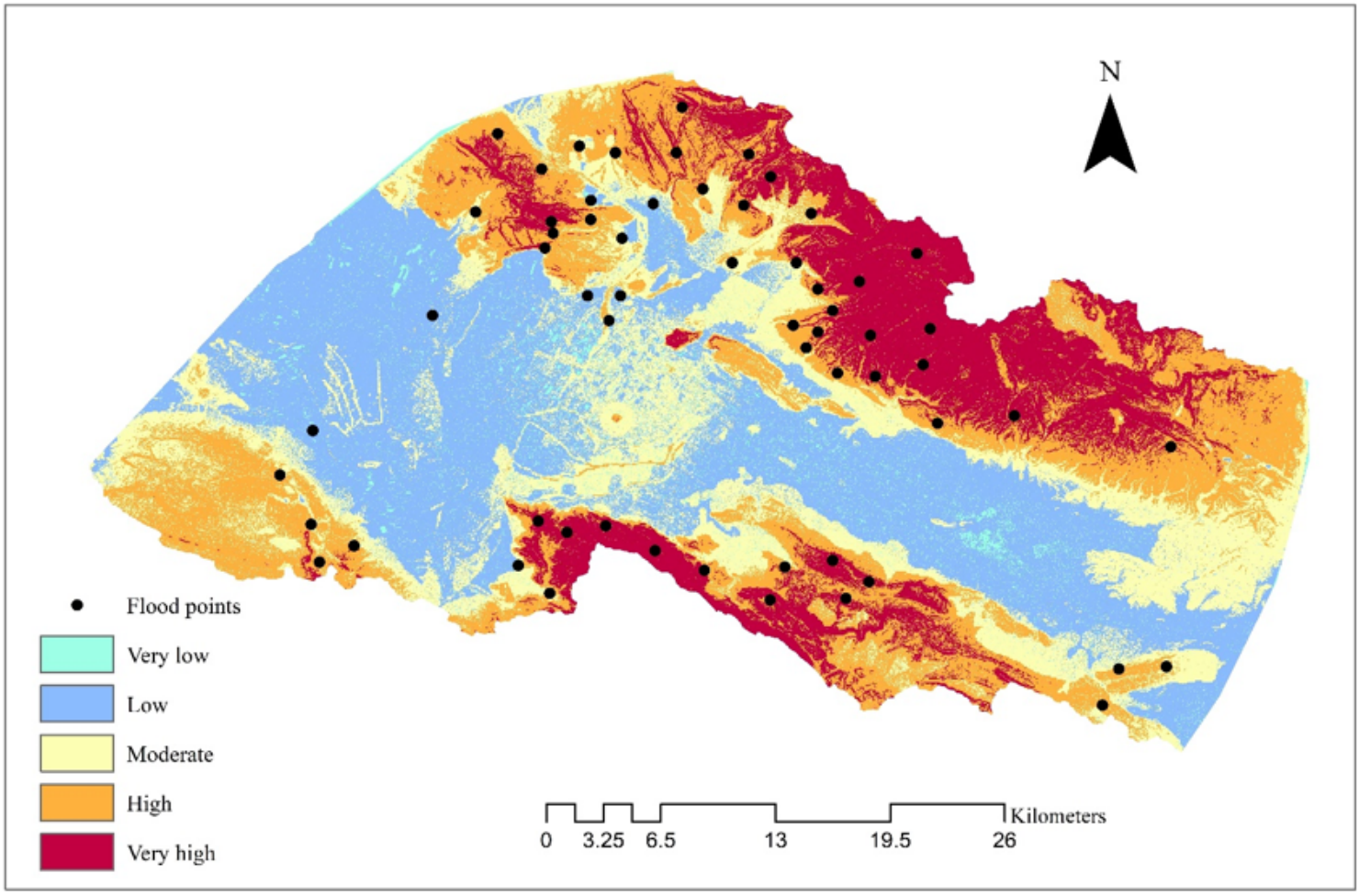

Figure 6

Distribution of GPS points of the flood hazard areas in the watershed

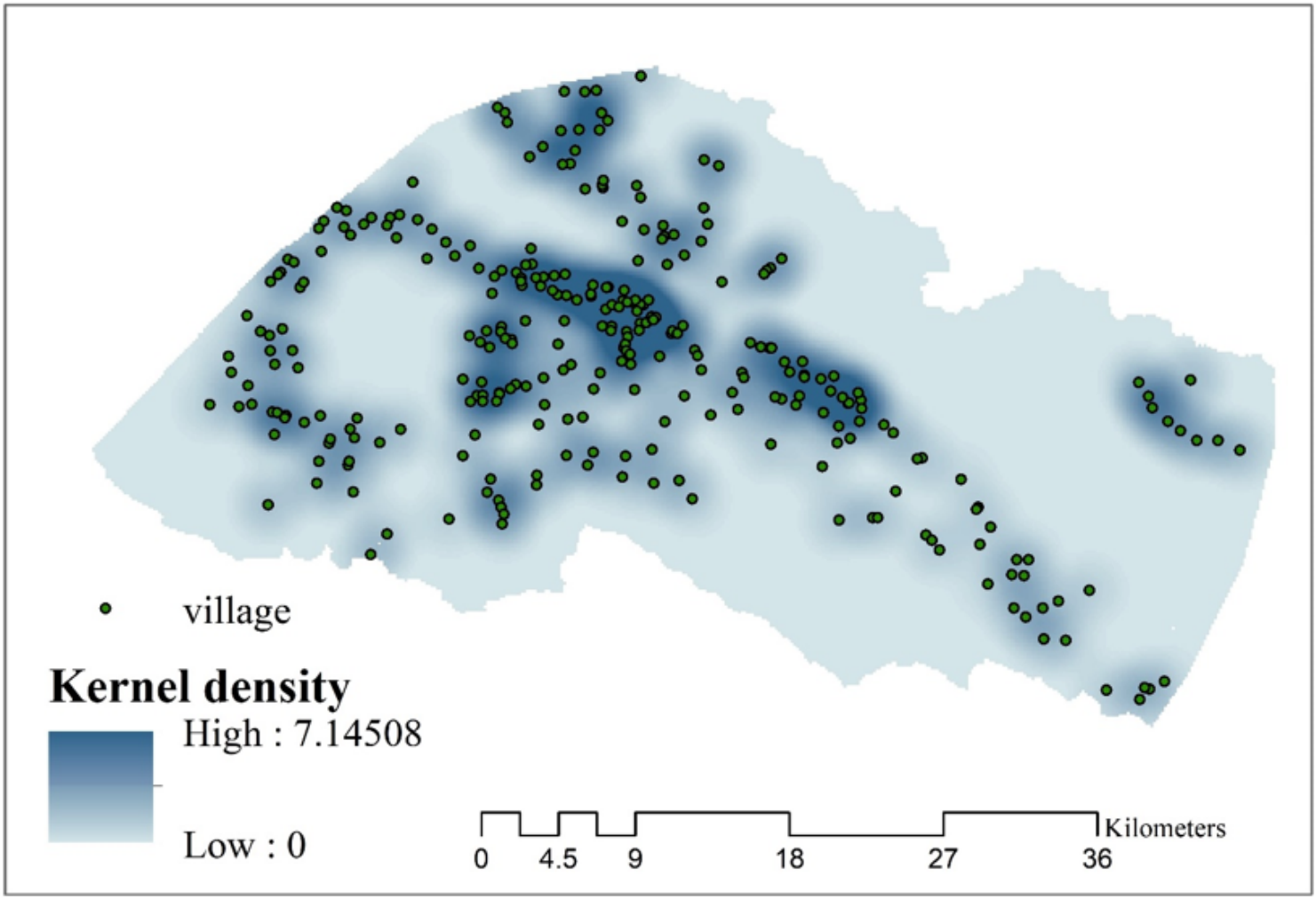

Figure 7

Kernel density estimation for residential areas

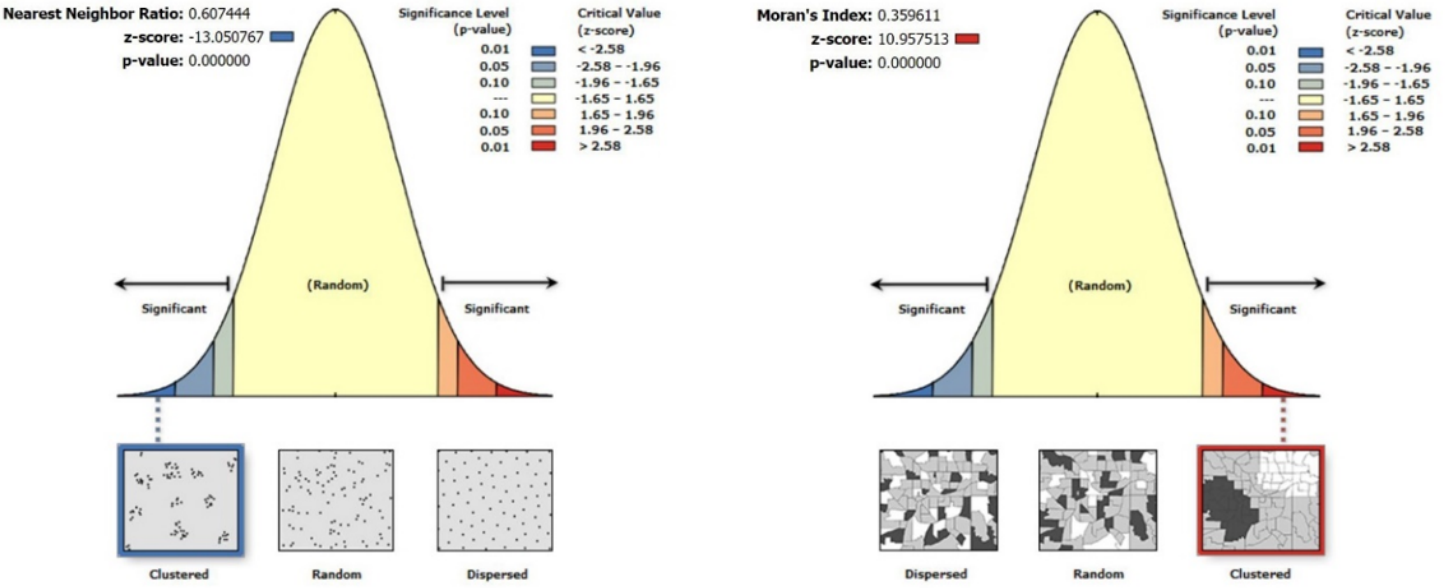

Figure 8

Spatial distribution pattern of weighted and unweighted residential areas

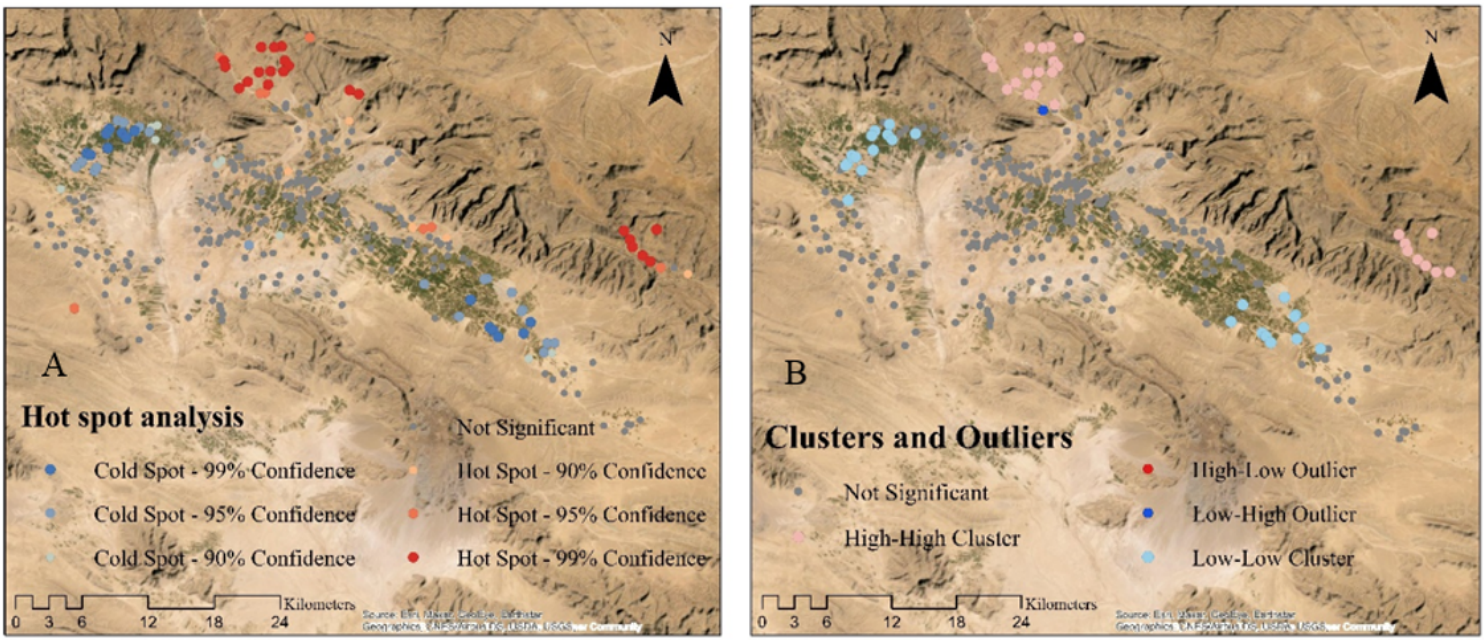

Figure 9

Identifying the high-risk and low-risk flood clusters, A: cluster and outlier analysis, B: hotspot analysis

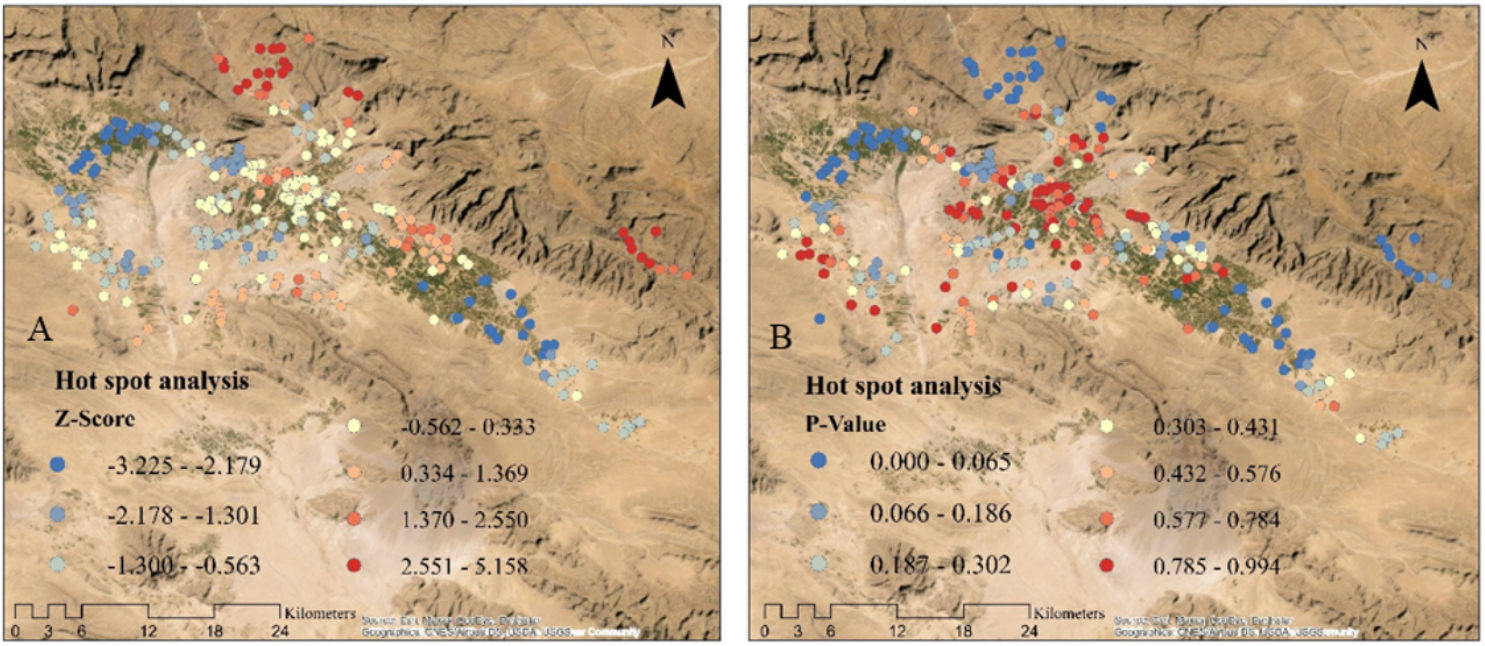

Figure 10

Hotspot analysis of flooding areas, A: Z-score, B: P-value

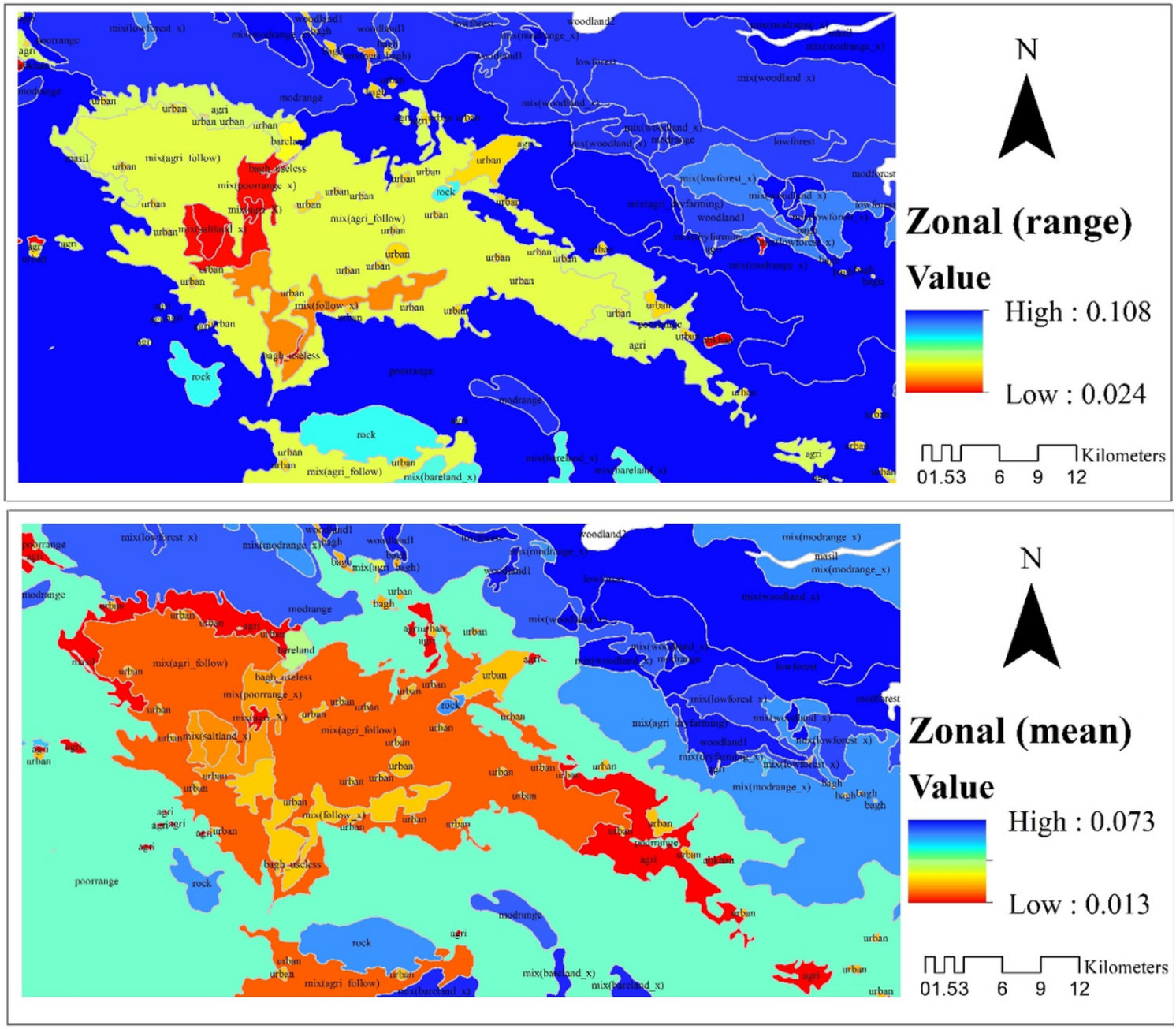

Figure 11

Zonation map of flooding rate based on the layer of Land cover

Supplementary Files

This is a list of supplementary files associated with this preprint. Click to download.

- AppendixA.docx